

Redox Processes in a Uranium Bis(1,1'-diamidoferrocene) Complex

Marisa J. Monreal, Colin T. Carver, and Paula L. Diaconescu*

Department of Chemistry and Biochemistry, University of California, Los Angeles, California 90095

Received March 8, 2007

Oxidation of a uranium(IV) bis(1,1'-diamidoferrocene) gives a compound which is best described as a mixed-valence bisferrocene complex in which uranium mediates the electronic communication.

Ferrocene, FcP_2 , and its derivatives are used more and more either as redox probes¹ or as substituents for ligands that coordinate to transition metals.² In both cases, the unique properties of ferrocene have been shown to influence the reactivity of the resulting compounds.^{3,4} If ferrocene is disubstituted in the 1,1' positions with donor atoms,⁵ a chelating ligand is generated in which iron will be placed relatively close to the metal center.⁶ Depending on the distance between iron and the metal center of interest, a direct interaction may be observed.⁷ We are interested in exploring the organometallic chemistry of uranium supported by ferrocene diamides and would like to assess if a direct uranium–iron interaction takes place and, if so, whether it influences the reactivity of the uranium center.

Because of its convenient synthesis and accessibility of a number of N-substituted derivatives, we chose $\text{fc}[\text{NHSi}(t\text{-Bu})\text{Me}_2]_2$ (fc = 1,1'-ferrocenylene)⁸ for our studies. The reaction between $\text{U}(\text{THF})_4$ ⁹ and $[\text{K}_2(\text{OEt}_2)_2]\text{fc}[\text{NSi}(t\text{-Bu})\text{Me}_2]_2$ in diethyl ether or toluene (Scheme 1) led to $\text{U}(\text{fc}[\text{NSi}(t\text{-Bu})\text{Me}_2]_2)_2$ (**1**), which could be purified by recrystallization from hexanes or Et_2O . The structure of the SiMe_3 analogue, $\text{U}(\text{fc}[\text{NSiMe}_3]_2)_2$, **1**^{SiMe3}, was determined by X-ray crystallography (Figure 1).¹⁰

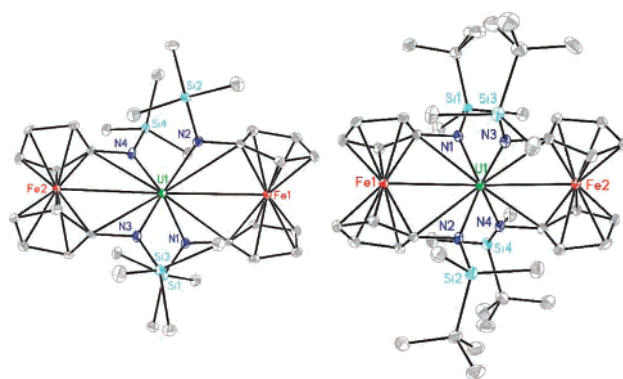


Figure 1. ORTEP representations (thermal ellipsoids at 35% probability) of **1**^{SiMe3} (left) and **1**-BPh₄ (right) (only one cation shown here; the other independent molecule in the unit cell, the anions, and the hydrogen atoms are omitted for clarity). U–Fe distances: 3.32 Å (av) in **1**^{SiMe3} and 2.90 Å (av) in the cationic compound.

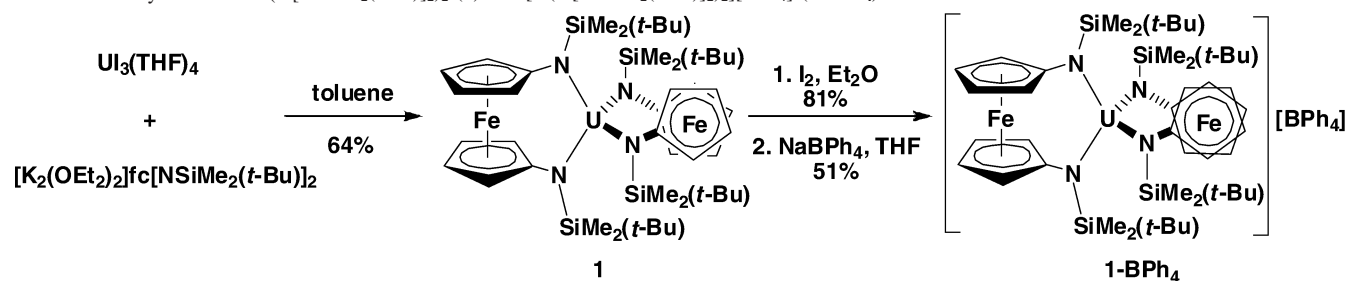
In compound **1** there are three redox-active metal centers: the two iron ions of the ferrocene ligands, which can undergo an Fe(II) to Fe(III) oxidation, and the uranium center, which, theoretically, can be oxidized from U(IV) to U(V).¹¹ All these processes could happen, in principle, around comparable oxidation potentials. To determine which processes are more likely, we undertook an electrochemical study of the free ligand, $\text{fc}[\text{NHSi}(t\text{-Bu})\text{Me}_2]_2$ (see Supporting Information), and compound **1** (Figure 2).

As expected, the cyclic voltammogram (CV) of the free ligand shows one reversible redox process, at -0.60 V vs $\text{Cp}_2\text{Fe}^{+/0}$ (see Supporting Information), consistent with the oxidation of Fe(II) to Fe(III). The CV of compound **1**, on the other hand, shows one irreversible reduction, one quasi-reversible, and two reversible redox processes at -3.26 , -2.54 , -0.69 , and 0.56 V versus $\text{FcP}_2^{+/0}$, respectively. Since the irreversible and quasi-reversible processes appear at potentials separated by no more than 0.7 V, it is very unlikely that they characterize both U(IV)/U(III) and U(III)/U(II) reductions. It is possible though that one of these waves corresponds to a ligand-based reduction while the other is

* To whom correspondence should be addressed. E-mail: pld@chem.ucla.edu.

- (1) Ulrich, S. Z. *Anorg. Chem.* **2005**, *631*, 2957–2966.
- (2) Atkinson, R. C. J.; Gibson, V. C.; Long, N. J. *J. Chem. Soc. Rev.* **2004**, *33*, 313–328.
- (3) Gregson, C. K. A.; Gibson, V. C.; Long, N. J.; Marshall, E. L.; Oxford, P. J.; White, A. J. P. *J. Am. Chem. Soc.* **2006**, *128*, 7410–7411.
- (4) Lorkovic, I. M.; Duff, R. R.; Wrighton, M. S. *J. Am. Chem. Soc.* **1995**, *117*, 3617–3618.
- (5) Siemeling, U.; Auch, T.-C. *Chem. Soc. Rev.* **2005**, *34*, 584.
- (6) Shafir, A.; Arnold, J. *J. Am. Chem. Soc.* **2001**, *123*, 9212.
- (7) Akabori, S.; Kumagai, T.; Shirahige, T.; Sato, S.; Kawazoe, K.; Tamura, C.; Sato, M. *Organometallics* **1987**, *6*, 2105–2109.
- (8) Shafir, A.; Power, M. P.; Whitener, G. D.; Arnold, J. *Organometallics* **2001**, *20*, 1365–1369.
- (9) Avens, L. R.; Bott, S. G.; Clark, D. L.; Sattelberger, A. P.; Watkin, J. G.; Zwick, B. D. *Inorg. Chem.* **1994**, *33*, 2248–2256.

- (10) Westmoreland, I.; Arnold, J. *Acta Cryst. E* **2006**, *62*, M2303–M2304; the structure of $\text{U}(\text{fc}[\text{NSiMe}_3]_2)_2$ reported here features a different space group, probably a consequence of different crystallization conditions.
- (11) Morris, D. E.; DaRe, R. E.; Jantunen, K. C.; Castro-Rodriguez, I.; Kiplinger, J. L. *Organometallics* **2004**, *23*, 5142–5153.

Scheme 1. Syntheses of $U(\text{fc}[\text{NSiMe}_2(t\text{-Bu})]_2)_2$ (**1**) and $[U(\text{fc}[\text{NSiMe}_2(t\text{-Bu})]_2)_2][\text{BPh}_4]$ (**1-BPh₄**)

associated with a U(IV)/U(III) process. We attribute the quasi-reversible process at -2.54 V to a U(IV)/U(III) reduction, noting that this value is higher than that for some $Cp^*_2U(IV)$ compounds.¹¹

Consequently, we assign the voltammetric wave at -3.26 V to a ligand-based reduction, which probably generates an unstable species on the voltammetric time scale. In order to gain additional information, we investigated the redox properties of the analogous Zr($\text{fc}[\text{NSiMe}_2(t\text{-Bu})]_2$)₂ (**2**). The CV for **2** shows one irreversible redox event at -3.49 V (see Supporting Information), which we assign to a Zr(IV)/Zr(III) process. Presumably, this event overlaps with the ligand-based reduction in **2**. The CV for **2** shows only irreversible processes, explaining the chemical instability of oxidized species.

In general, two ferrocene ligands coordinated to a metal center will display individual oxidation events if electronic communication between the two iron centers is possible.¹² Noting that such an electronic communication can occur either through the cyclopentadienyl amides or through a direct uranium–iron interaction, it is reasonable to assume that the two reversible processes we observe, at -0.69 and 0.56 V (Figure 2), correspond to the two Fe(II)/Fe(III) oxidations (with a comproportionation constant, K_c , of 1.55×10^{21}).¹³ The difference between the two Fe(II)/Fe(III) oxidations indicates a strong electronic communication between the ferrocene fragments, much stronger than in the zirconium compound **2** (0.21 and 0.90 V, $K_c \approx 10^{11}$). To conclude the cyclic voltammetry studies, it seems that the U(IV)/U(V) oxidation happens outside the experimental range used for our studies.

In order to establish if any of the species observed electrochemically are chemically stable, we undertook the chemical oxidation of compound **1**. The reaction of **1** with mild oxidants such as I_2 gave a solid which could be easily transformed into $[U(\text{fc}[\text{NSi}(t\text{-Bu})Me_2]_2)_2][\text{BPh}_4]$, **1-BPh₄**

(Scheme 1), by reaction with $NaBPh_4$. Similarly, oxidation with $AgOTf$ led to an intermediate triflate compound, which could be converted into **1-BPh₄** (Figure 1). Further oxidation of **1-BPh₄** was not possible with $AgOTf$. Chemical oxidation of **2** led to the removal of a ligand from Zr, observation consistent with the CV for **2**, which shows (see Supporting Information) multiple chemical species depending on the acquisition conditions.

The X-ray crystal structure of **1-BPh₄** indicates that the solid consists of isolated cations and anions, and no intermolecular interactions were observed. In both **1** and **1-BPh₄** the two ferrocene ligands adopt an almost perpendicular orientation, as indicated by the torsion angles N1–Fe1–Fe2–N3, which are 88.7° and 75.3° for **1** and **1-BPh₄**, respectively. Surprisingly, there is not much change in the U–N or Fe–C distances between the two compounds: in compound **1**, the averaged U–N and Fe–C distances are 2.264 and 2.070 Å, respectively, while in **1-BPh₄** they register 2.268 and 2.077 Å, respectively. These Fe–C distances are similar to distances found in ferrocenium compounds.¹⁴ The only distances that change significantly between compounds are the U–Fe distances: 3.325 Å in **1** and 2.961 Å in **1-BPh₄**. All distances discussed here have similar values for both sides of each compound, pointing toward symmetrical halves of the molecule. In solution, 1H NMR spectroscopy indicates a symmetrical environment around the uranium center since only one set of ligand peaks is observed.

Since X-ray crystallography and 1H NMR spectroscopy studies show that **1-BPh₄** adopts a symmetrical structure both in the solid state and solution, we decided to use other characterization methods to gain insight into its electronic structure. Temperature-dependent magnetization studies show that the room-temperature magnetic moment values for both compounds are very similar (Figure 3, $2.41 \mu_B$ for **1** and $2.61 \mu_B$ for **1-BPh₄**). However, at low temperatures, compound **1** shows typical U(IV) behavior (as the temperature decreases, nonmagnetic states are populated, leading to a small magnetic moment originating from TIP—temperature-independent paramagnetism),¹⁵ whereas **1-BPh₄** shows a decrease of the magnetic moment value from $3.01 \mu_B$ at 40 K to $2.70 \mu_B$ at 4 K.

For uranium compounds, a smaller value of the room-temperature magnetic moment than the one calculated for

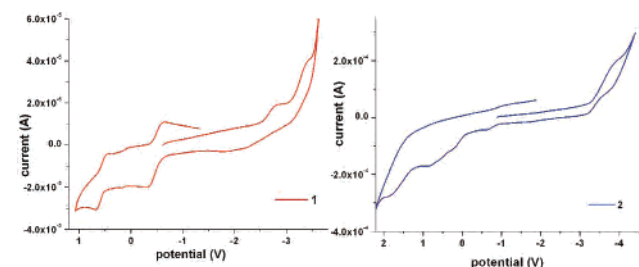


Figure 2. Cyclic voltammogram of $U(\text{fc}[\text{NSiMe}_2(t\text{-Bu})]_2)_2$ (**1**) and $Zr(\text{fc}[\text{NSi}(t\text{-Bu})Me_2]_2)_2$ (**2**) in 0.1 M $[^nBu_4N][PF_6]$ in THF, referenced versus $Cp_2Fe^{+/0}$.

(12) Xu, G. L.; Crutchley, R. J.; DeRosa, M. C.; Pan, Q. J.; Zhang, H. X.; Wang, X.; Ren, T. *J. Am. Chem. Soc.* **2005**, *127*, 13354–13363.

(13) Kaim, W.; Lahiri, G. K. *Angew. Chem., Int. Ed.* **2007**, *46*, 1778.

(14) Mammiano, N. J.; Zalkin, A.; Landers, A.; Rheingold, A. L. *Inorg. Chem.* **1977**, *16*, 297–300.

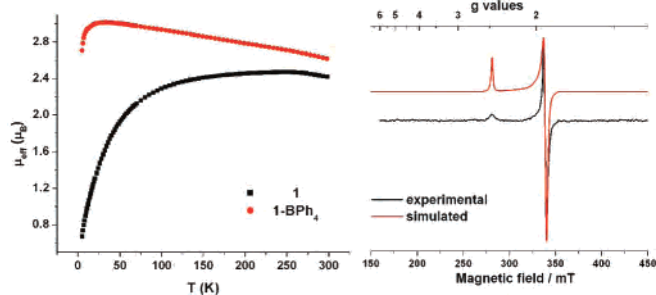


Figure 3. Left, magnetic moment (μ_{eff}) versus T for **1** and **1-BPh₄**; right, EPR spectrum of **1-BPh₄** recorded in a CH₃CN/toluene (1:1) solution at 4.2 K (bottom) and simulated (top).

the free ion is a consequence of partly quenching the orbital-angular momentum either because of a lower symmetry or higher covalency than for the free ion ($^3\text{H}_4$ for U(IV)).¹⁶ It could be inferred that compound **1** shows an appreciable degree of covalency since its magnetic moment at room temperature (2.50 μ_B) is significantly smaller than expected (3.58 μ_B for the free ion). This interpretation is consistent with the fact that the Fe(II) orbitals are diffuse and overlap well with the uranium orbitals and support a direct uranium–iron interaction (see Supporting Information for DFT calculation details).

The temperature dependency of μ_{eff} for **1-BPh₄** is best interpreted as being a consequence of interacting U(IV) and Fe(III) centers, although details of this interaction are difficult to assess because of the complexity of uranium magnetic properties.

One method used to characterize the electronic communication in bisferrocene compounds is EPR spectroscopy.¹⁷ The spectrum displayed in Figure 3 is representative for compound **1-BPh₄** and it shows, based on Δg ($\Delta g = g_{\parallel} - g_{\perp}$, ca. 0.4), that the electron is completely delocalized over the two iron centers on the EPR time scale.¹⁸ Compounds in which there are localized Fe(II) and Fe(III) centers show values for Δg higher than 1.4 (in ferrocenium triiodide $\Delta g = 3.09$).¹⁹ The EPR data thus allow the estimate of a lower limit for the rate of electron transfer of ca. 10^{10} s^{-1} .

Other methods for probing the electronic communication in mixed-valence compounds are NIR and IR spectroscopy. Compound **1** presents in the NIR spectrum (Figure 4) relatively narrow bands with $\epsilon \approx 10^2 \text{ M}^{-1} \text{ cm}^{-1}$, consistent with f–f transitions. The NIR spectrum of compound **1-BPh₄**, on the other hand, shows (Figure 4) an absorption

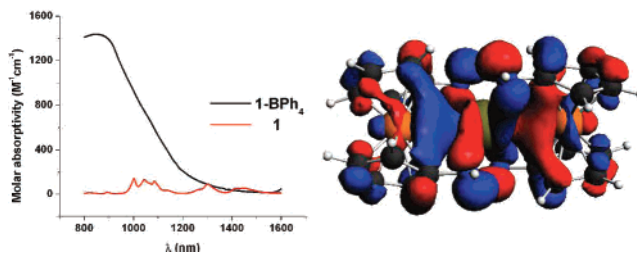


Figure 4. Left, NIR (1 mM CH₂Cl₂) spectra of **1** and **1-BPh₄**; right, HOMO of the Th(fc[NH]₂)₂ cation.

band with $\epsilon \approx 10^3 \text{ M}^{-1} \text{ cm}^{-1}$, consistent with an intervalence charge-transfer transition. The parameter²⁰ V_{ab} of 2085 cm^{-1} is characteristic of systems strongly coupled,²¹ supporting the CV and EPR data interpretation. The IR spectra for **1-BPh₄** (see Supporting Information) show two bands, at 818 and 840 cm^{-1} , that can be assigned to the cyclopentadienyl perpendicular C–H bending vibrations, indicating that both ferrocene and ferrocenium centers are present.²² IR data thus give the upper limit of the electron-transfer rate of ca. 10^{13} s^{-1} .

DFT calculations (Figure 4 and Supporting Information) performed on thorium and zirconium model systems show that electronic communication between iron and thorium or zirconium is possible as a consequence of direct orbital interactions. For the thorium bisferrocene cation model system, additionally, the HOMO consists of an f orbital interacting with both iron centers at the same time, which might explain the different behavior between the uranium and zirconium bisferrocene complexes.

In conclusion, a mixed-valent bisferrocene compound was synthesized and its characterization supports a uranium-mediated electronic communication between the two iron centers. We are currently investigating why uranium is a better electronic mediator for the two iron centers than zirconium.

Acknowledgment. The authors thank Prof. Karsten Meyer for discussions, Dr. Robert Taylor for help with EPR, and Prof. Jeffrey Zink for allowing the use of the UV–vis–NIR spectrometer. This work was supported by the UCLA and the UC Energy Institute (EST grant).

Supporting Information Available: Experimental details for compound syntheses, X-ray crystal structures for compounds **1** and **1-BPh₄**, CVs for the free ligand, **1-BPh₄**, and **2**, spectra, and DFT calculation details. This material is available free of charge via the Internet at <http://pubs.acs.org>.

(15) Stewart, J. L.; Andersen, R. A. *New J. Chem.* **1995**, *19*, 587.

(16) Castro-Rodríguez, I.; Olsen, K.; Gantzel, P.; Meyer, K. *J. Am. Chem. Soc.* **2003**, *125*, 4565–4571.

(17) Webb, R. J.; Geib, S. J.; Staley, D. L.; Rheingold, A. L.; Hendrickson, D. N. *J. Am. Chem. Soc.* **1990**, *112*, 5031–5042.

(18) Nakashima, S.; Masuda, Y.; Motoyama, I.; Sano, H. *Bull. Chem. Soc. Jpn.* **1987**, *60*, 1673–1680.

(19) Prins, R.; Reinders, F. J. *J. Am. Chem. Soc.* **1969**, *91*, 4929.

IC700457H

(20) Patra, S.; Miller, T. A.; Sarkar, B.; Niemeyer, M.; Ward, M. D.; Lahiri, G. K. *Inorg. Chem.* **2003**, *42*, 4707–4713.

(21) Hush, N. S. *Coord. Chem. Rev.* **1985**, *64*, 135–157.

(22) Kramer, J. A.; Hendrickson, D. N. *Inorg. Chem.* **1980**, *19*, 3330–3337.